Landes Bioscience www.landesbioscience.com

Supplemental Material to:

Mark A. Badeaux, Collene R. Jeter, Shuai Gong, Bigang Liu, Mahipal V. Suraneni, Joyce Rundhaug, Susan M. Fischer, Tao Yang, Donna Kusewitt, and Dean G. Tang

In vivo functional studies of tumor-specific retrogene NanogP8 in transgenic animals

Cell Cycle 2013; 12(15)
http://dx.doi.org/10.4161/cc.25402

http://www.landesbioscience.com/journals/cc/article/25402

SUPPLEMENTAL RESULTS

Other developmental defects in K14-NanogP8 Tg mice: Thymic atrophy and cataracts

We also analyzed the thymi in two P5 and four P14-P17 L1 Tg animals. One P5 thymus was substantially smaller than the WT counterpart with extensive apoptosis (Figure S3C). Histologically, the distinct separation of thymic cortex and medulla seen in the WT P5 mouse was lacking in the P5 Tg (Figure S2C, top). IHC staining demonstrated that K14-expressing epithelial cells were located exclusively in the medulla of WT P5 thymus but were scattered throughout the Tg thymus (Figure S2C). NanogP8-positive cells were found in a similar pattern to K14 throughout the P5 Tg thymus (Figure S2D). These observations suggest that constitutive overexpression of NanogP8 in K14-expressing thymic epithelial cells disrupts normal thymus development, at least in some animals, which requires the differentiation of a common bipotential progenitor cell expressing EpCAM and Plet-1/MTS24 into thymic epithelial cells of the cortex and medulla (1,2). Thymi in older mice varied from essentially normal in appearance to moderately disorganized (Figure S2E; data not shown). Disorganization was characterized by the presence of scattered islands of medullary tissues instead of a single central medulla and, in most TG mice, there were unusual duct-like structures (not shown). NanogP8-positive cells were observed in both cortex and medulla (Figure S2E).

Both lines of Tg mice developed cataracts (Figure S3A). High NanogP8 expression in L1 led to cataract development by one month of age in all mice, whereas lower levels of NanogP8 expression in L3 (Figure 1F) led to the later development (≥3 months of age) of cataracts in ~40% of the animals. L3 animals that expressed very low levels of NanogP8 (Figure 1F) did not develop cataracts. WT lenses exhibited the typical pattern of lens epithelial cell migration and differentiation (Figure S3B-C). However, the lenses of Tg mice with cataracts exhibited severe degenerative changes (Figure S3B-D). There was clumping, vacuolation, and liquifaction of cortical and nuclear lens proteins. The normal pattern of lens epithelial cell differentiation was lost, and no clearly defined bow region was present (Figure S3B). Moderate numbers of nucleated and vacuolated epithelial cells, positive for NanogP8, were observed within the remains of the lens and at the posterior lens surface

(Figure S3, B and D). Preliminary studies with β-crystalline staining suggested abnormal distribution of β-crystalline in the Tg lens (data not shown).

SUPPLEMENTAL METHODS

Animal housing and care

Animal-related studies were approved by the M.D Anderson Cancer Center Institutional IACUC committee (ACUF 08-05-08132). Animal housing and experimental procedures were conducted in an animal facility accredited by the American Association for the Assessment and Accreditation of Laboratory Animal Care (AAAALAC), in accordance with Institutional Animal Care and Use Committee (IACUC) guidelines. Mice were fed *ad libitum* unless otherwise noted.

Harvest of murine organs

Mice were sacrificed, and internal organs or skin samples were removed quickly, placed directly into microcentrifuge tubes, and were then immersed in liquid nitrogen (for Western blot). Alternatively, the organs were placed into cassettes and immersed in 10% formalin for 24-48 h followed by immersion in 70% ethanol (for immunohistochemistry). Organs were embedded in paraffin, sectioned, and placed on glass slides. Organ protein lysate was made by cryopulverizing the tissue then immersing the powder in chilled lysis buffer containing 25 mL/mL protease inhibitor cocktail (Sigma). The lysate was centrifuged at 16,000 *g* for two min at 4°C and the supernatant was used to perform Western blot.

Western blotting analysis

Protein samples were loaded in equal amount in each well of a 12.5% polyacrylamide gel and electrophoresed until the protein ladder was fully resolved. Proteins were transferred to nitrocellulose membrane (Biorad), which was blocked using 4% milk in TBST (Tris-buffered saline with Tween). Primary antibodies (Table S1) were diluted in 4% milk/TBST and were incubated on the membrane at 4°C overnight. Appropriate horseradish peroxidase-conjugated secondary antibodies were added at a 1:2000 dilution using 4% milk/TBST as a diluent and incubated for 1 h at room temperature. Luminescence was produced using Western lightning ECL plus detection reagent (Perkin Elmer).

Immunohistochemistry (IHC)

Tissues were embedded in paraffin blocks, and 4-μm sections were cut. Slides were deparaffinized in xylene or a xylene substitute (CitraSolv; LLC, Danbury, CT) for 2 – 5 min. Tissues were hydrated in a series of alcohols and water before undergoing antigen retrieval by microwaving in 10 mM citrate buffer. After antigen retrieval, endogenous peroxidase activity was quenched with hydrogen peroxide (3% for 10 min), and sections were blocked with 10% normal goat serum in phosphate-buffered saline (PBS) for 30 min. Primary antibodies (Table S1) were applied for times ranging from 30 min at room temperature to overnight at 4°C. Slides were washed twice for 5 min each in PBS before application of the secondary antibody. For most antibodies, slides were incubated with the secondary antibodies for 30 min. Staining was developed by incubating sections with diaminobenzidine and tissue sections were counterstained with hematoxylin.

To identify proliferating cells, we used an anti-Ki-67 antibody (Dako). To identify apoptotic cells, we used an antibody raised against active-caspase-3 (R&D Systems), or alternatively, we utilized the TdT-FragEL DNA Fragmentation Kit (Calbiochem), aka TUNEL staining.

Immunofluorescence staining

Regular formalin fixed paraffin embedded tissue sections (4 μm) were de-paraffinized in xylene and then hydrated in graded alcohols to water. Endogenous peroxidase activity was blocked with 3% H_2O_2 in water for 10 min. Antigen retrieval was performed with 10 mM citrate buffer (pH 6.0) for 15 min in a microwave oven followed by a 20-min cool down and thorough wash. Slides were incubated with Biocare Blocking Reagent (#BS966M with casein in the buffer; Biocare, Concord, CA) for 10 min to block non-specific antibody binding. After draining, slides were incubated with Background Sniper (Biocare; cat#BS966H) for 15 min. Slides were washed in TBS buffer and then incubated with various primary antibodies (at 50 – 1000 dilutions as determined from pilot experiments) for 1 h at room temperature. Slides were washed in phosphate buffer twice and then incubated in goat-anti-rabbit IgG or donkey-anti-goat IgG (Life technologies) at a 1:500 dilution for 1 h at room

temperature. After thorough washing, slides were incubated in DAPI (1mg/ml) for 10 min, mounted in PermaGold Antifade Mounting Agent (Invitrogen), and covered with coverslips. IF images were acquired on either an Olympus BX40 epifluorescence microscope or a Zeiss confocal microscope.

In vitro wound healing (scrape) assays

Keratinocytes freshly prepared from newborn WT or L1 Tg mice were plated in 60-mm dishes on collagen and laminin substrates and allowed to attach for 4-6 h. The medium was changed to calcium-free KBM Gold (Lonza) supplemented with 0.05 mM calcium. Upon confluence, cells were treated with mitomycin C to block cell proliferation. A cell-free region (i.e., the wound) was made by scraping the monolayer with a pipet tip, and cells were allowed to re-enter the void by migration. Measurements were made 12 h post-scrape/wound by counting the number of cells that migrated into the scraped area, and images were captured using an IX71 Olympus inverted microscope with DP71 camera.

Clonal assays

Swiss 3T3 cells were grown to confluence, irradiated with 6 Gy of X-ray, and re-seeded at 1/3 confluence in 60-mm dishes containing 5 mL of DMEM supplemented with FBS. 24 h later, 2.5 x 10^3 adult keratinocytes freshly prepared from adult (2-3 months old) mice were plated on the feeder layer in KBM Gold media (Lonza) with calcium supplementation to facilitate attachment. Media were changed to KBM Gold without exogenous calcium 8 h later, and was replaced three times a week thereafter for two weeks. Recombinant bone morphogenetic protein 5 (Bmp5) was added to the media of relevant wells at a final concentration of 0.05 mg/mL, beginning with the first medium change.

To stain the colonies, culture medium was removed and dishes were washed twice in PBS. 10% buffered formalin was added to the plates, which were allowed to incubate overnight at 4°C. Next day, formalin was removed and plates were again washed once with PBS and then 0.4% Rhodamine B was added to each plate. Plates were then incubated for 30 min, washed with water for 5-10 seconds, and allowed to air dry, after

which time colonies were counted. Images were captured using an Olympus CK 40 SLP inverted microscope with DP11 camera.

Quantitative RT-PCR analysis

RNA was extracted using the RNeasy mini kit (Qiagen) with on-column DNase treatment to remove contaminating genomic DNA, and sample quality was verified using the Agilent Bioanalyzer. Reverse transcription was carried out using the SuperScript III First-Strand Synthesis System (Invitrogen). Real-time primers were designed using NCBI's Primer Blast online software (http://www.ncbi.nlm.nih.gov/tools/primer-blast/), and genes to be analyzed were chosen by searching the literature for ChIP studies in which Nanog binding was assayed. Genes (see Table S2 for primer information) to which Nanog bound near the promoter region in both mouse and human systems were given preference as likely targets of human NanogP8 protein binding to regions of the mouse genome.

In vivo wound healing experiments

Epidermal abrasion experiments were performed by first shaving mice 2 days prior to wounding. Hair stubble was removed by application of Nair just prior to epidermal abrasion. Mice were anesthetized by inhalation of isofluorane. A felt cylinder was attached to an electric handheld rotary tool, and wounds were made superficially such that the dermis was just visible. Removal of epidermis and integrity of hair follicles were both confirmed histologically on randomly selected samples.

SUPPLEMENTAL REFERENCES

1 Rossi SW, Jenkinson WE, Anderson G, and Jenkinson EJ. Clonal analysis reveals a common progenitor for thymic cortical and medullary epithelium. *Nature* 2006; 441: 988-991.

2 Bleul CC, Corbeaux T, Reuter A, Fisch P, Mönting JS, and Boehm T. Formation of a functional thymus initiated by a postnatal epithelial progenitor cell. *Nature* 2006; 441: 992-996.

SUPPLEMENTAL FIGURE LEGEND

Figure S1. The P5 L1 K14-NanogP8 skin is atrophic.

Shown are representative immunofluorescence images of K14 staining in the skins of two P5 WT (top) and L1 Tg (bottom) animals, respectively. The epidermal side of all skin strips is shown. It is clear that the Tg skins are much thinner and lack the hypodermis. Original magnifications: x100.

Figure S2. Skin phenotypes in P15 L1 Tg animals

(**A**) The P15 WT and L1 Tg (i.e., L1-F1 Tg#2; see Fig. 2B) animals. Note the smaller body size and the ocular abnormalities in the Tg animal.

(**B**) Composite H & E images of the P15 WT and L1 Tg skin (original magnifications, 40x). Note that the Tg skin (bottom) was thinner than the WT skin (top) with reduced numbers of hair follicles and hair shafts (above the epidermis) and an apparent lack of the hypodermis (the fatty layer beneath the hair bulbs).

(**C**) H & E and IHC staining for the molecules indicated. Hyperkeratosis can still be noted by comparing images in g and h. Original magnifications: x100.

(**D**) Quantification of Ki-67^{+} cells in P15 WT and L1 Tg epidermis (500 cells counted for each genotype).

Figure S3. Developmental abnormalities in other organs in the L1 Tg mice

(A) Lack of milk in L1 NanogP8 Tg stomach. Shown are representative H & E and NanogP8 IHC images of a P5 WT (a,c,e) and Tg (b,d,f) stomach. Note the expression of NanogP8 only in the Tg stomach.

(B) The P5 Tg tongue lacks filiform papillae. The P5 WT (a,c) and Tg (b,d) sections were used in H & E (a,b) and IHC staining for NanogP8 (c,d). Arrows in a indicate developing filiform papillae. Note the expression of NanogP8 only in the Tg tongue.

(**C-E**) Abnormal thymus development. C-D. Smaller P5 Tg thymus and abnormal K14 expression pattern (C) and NanogP8 expression (D). E. NanogP8 staining in a P15 thymus.

Figure S4. Cataracts in the eyes of Tg animals

(**A**) Gross images showing ocular abnormalities in a 1 month-old L1 (top) and a 3 month-old L3 (bottom) animal.

(**B**) Representative H & E images of a WT and a L1 Tg eye with the indicated areas.

(**C**) Histological features and NanogP8 staining in a WT eye (4 months). In a, the orientation of the lens is indicated: an, anterior (facing the iris and cornea, shown in b); p, posterior (facing the retina); l, lateral. Note that the posterior (post.) region of the lens generally lacks nucleated cells (c-d) although such cells were observed in the lateral (lat.) region (e). NanogP8 was not detected in WT eyes (f). The original objectives (4x, 10x, and 20x) are indicated.

(**D**) Histological features and NanogP8 staining of left (a-f) and right (g-j) eyes of an 8 month-old L3 Tg mouse. Orientations and other labels are the same as in C. The left eye was characterized by prominent presence of NanogP8-expressing nucleated epithelial cells in the posterior lens (c-f) whereas the right lens showed a completely degenerate phenotype (g-j).

Figure S5. Similar responses of WT and Tg epidermis to TPA

(**A**) TPA treatment induced similar hyperplastic changes in the WT and L1 Tg skin. Shown are representative H & E images (n =3 for both wt and tg). TPA was applied every other day for two weeks.

(**B**) Ki-67 staining in the IFE and HFs of mice treated with TPA. The proliferative response between WT and the L1 Tg skin in response to phorbol ester stimulation appears identical.

Figure S6. Abnormal Sox9 and Lgr6 expression in the P5 L1 Tg skin

(**A**) Sox9 immunostaining in P5 WT and L1 Tg skins. Shown are 3 representative immunofluorescence images, respectively, from one WT (top) and Tg (bottom) animal each. Identical results were obtained in another two pairs of animals studied. Original magnifications: x200.

(**B**) Lgr6 immunostaining in 3 pairs of P5 WT and L1 Tg skins. Shown are representative immunofluorescence images from 3 WT (top) and Tg (bottom) animals. Original magnifications: x200.

Table S1 . Primary antibodies used in the current study

Antibody	Host	Clonality	Company	Catalog #
Anti-human Nanog	rabbit	polyclonal	Cell Signaling	3580
Anti-mouse Nanog	rabbit	polyclonal	Abcam	70482
Anti-human Nanog	goat	polyclonal	R&D Systems	AF1997
Anti-human c-Myc	rabbit	monoclonal	Epitomics	1472-1
Anti-Beta actin	rabbit	polyclonal	Cell Signaling	4967
Anti-mouse Lrig1	goat	polyclonal	R&D Systems	AF 3688
Anti-mouse CD 34-FITC	mouse	monoclonal	BD Pharmingen	560942
Anti-mouse CD 49f	rat	monoclonal	BD Pharmingen	555736
Anti-mouse activated caspase 3	rabbit	polyclonal	R&D Systems	MAB8835
Anti-mouse Ki67	rat	monoclonal	Dako	M7249
Anti-mouse keratin 1	rabbit	polyclonal	Covance	PRB-165P
Anti-mouse keratin 6	rabbit	polyclonal	Covance	PRB-169P
Anti-mouse keratin 10	rabbit	polyclonal	Covance	PRB-159P
Anti-mouse keratin 13	mouse	monoclonal	Covance	16112
Anti-mouse keratin 14	rabbit	polyclonal	Covance	PRB-155P
Anti-mouse Protein Kinase C -alpha	rabbit	polyclonal	Santa Cruz	sc-208
Anti-BrdU	mouse	monoclonal	BD Pharmingen	347580
Anti-human Sox9	rabbit	polyclonal	Santa Cruz	sc-20095
Anti-human Lrg6	goat	polyclonal	Santa Cruz	sc-48236

Table S2. Real-time PCR primers used in gene expression studies

Gene	Forward Primer (5′--3′)	Reverse Primer (5′--3′)	Product Size	Annealing Temperature
Bmp2	TCCAGAGCTGGGCCGCAAGA	GAAGAAGCGCCGGGCCGTTT	322bp	60
Bmp4	TGCCATTCGGAGCGACGCAC	CGCGTGGCCCTGAATCTCGG	244bp	60
Bmp5	GCCTCTCCCAATGGGTATGCGC	TGCTTCTCCATGTGGAATCTGGGT	225bp	58
Bmp7	CGGACAGGGCTTCTCCTACCCC	AACCGGAACTCCCGATGGTGGT	177bp	60
Cdk6	CACGGACGGACAGAGAAACCAAGC	CACAGCGTGACGACCACCGA	295bp	59
Dlx3	TACTCGGGCCAGCCCTACGG	CGTTCGCGGCTTTCGGACCT	252bp	59
Fgfr2	CCAGGGATTGGCACTGTGACCA	ACTGCAACTCTAGCGATTCCCCG	205bp	58
Frizzled 10	GGTCACGAGAACCAGCGCGA	ATCCGAGCCGTTGTTGGGTGC	300bp	59
Gli1	AGACGCACCTTCGGTCGCAC	CCCCTCGATGCCGCTTGGTC	243bp	59
Igfbp2	CGCTACGCTGCTATCCCAACCC	GGTCCAACTCCTGCTGGCAAGG	363 bp	59
Jmjd1a	TCCCCAGGCAGCCAATTCTCCA	TGGCTGTGGAGCAGACTCCAGT	274bp	59
Jun	GACGGACTTGGCCAACCCGG	GCAAAAGTTCGCTCCCGGCC	292bp	59
Klf5	CCCACCTCCGTCCTATGCCGC	GCGGGTCAGCTCATCCGACC	298bp	59
Patched1	ACCACAGGGCTATGCTCGCTCT	GGCACGGCAAACCGGACGAC	295bp	59
Pten	TCCCAGACATGACAGCCATCATCAA	GCTGTGGTGGGTTATGGTCTTCAAA	300bp	57
Wnt3	CAGTCACACGCTCCTGCGCT	GAGCGCGTACTTAGCCCGCA	419bp	59

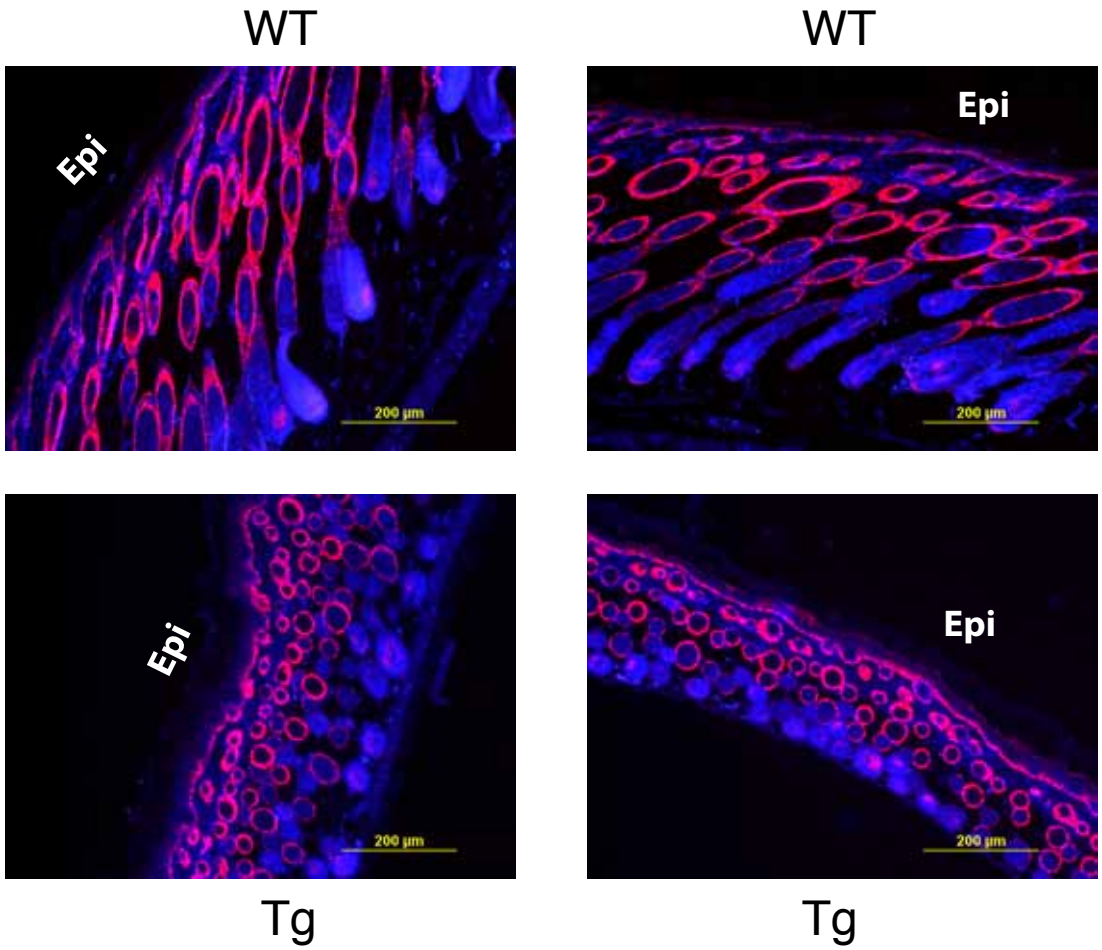
WT
WT
Epi
Epi
200 µm
200 µm
Epi
Epi
200 µm
200 µm
Tg
Tg

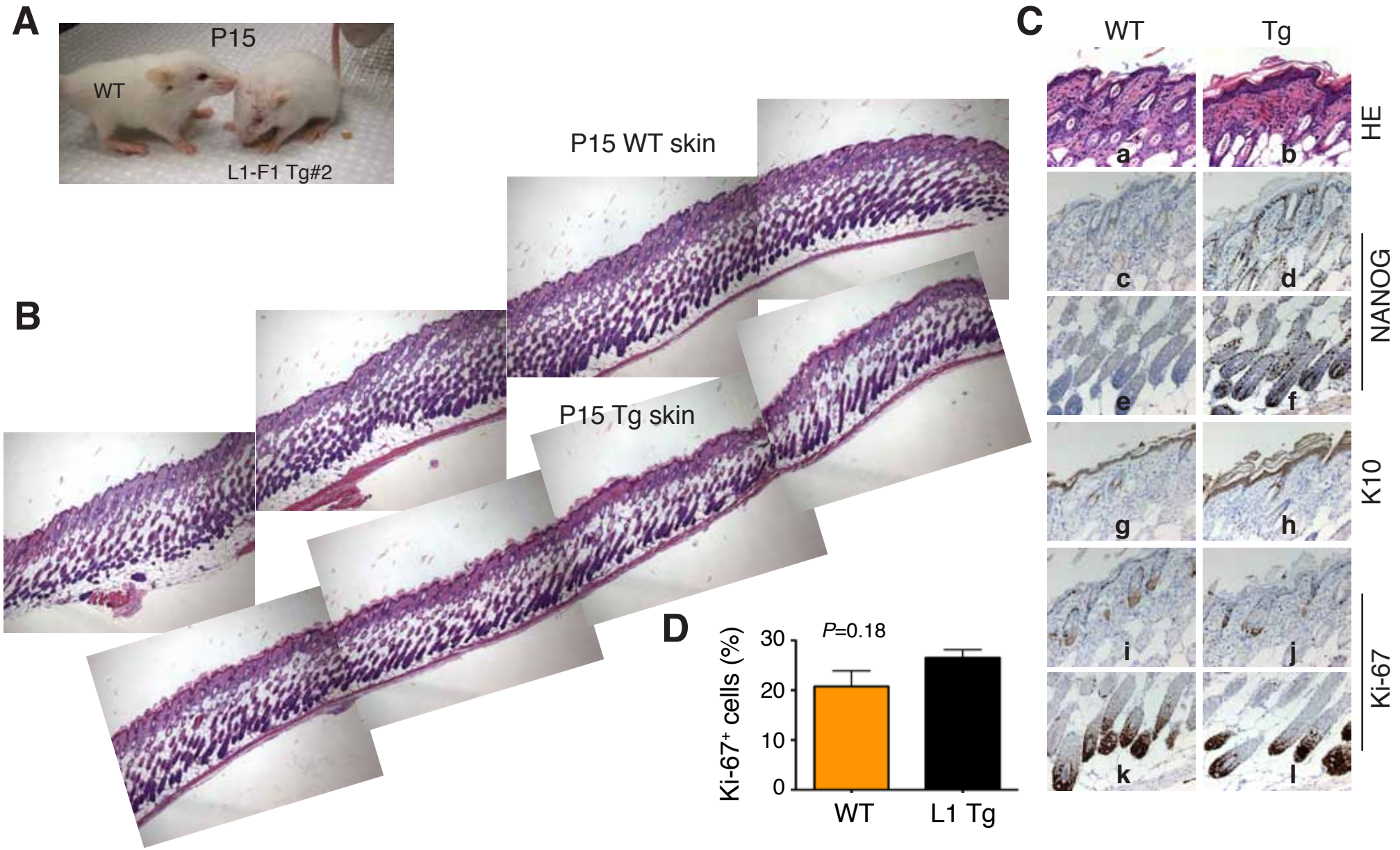
A
P15
WT
L1-F1 Tg#2
B
P15 WT skin
P15 Tg skin
C
WT
Tg
HE
NANOG
K10
Ki-67
a
b
c
d
e
f
g
h
i
j
k
l
D
P=0.18
Ki-67+ cells (%)
30
20
10
0
WT
L1 Tg

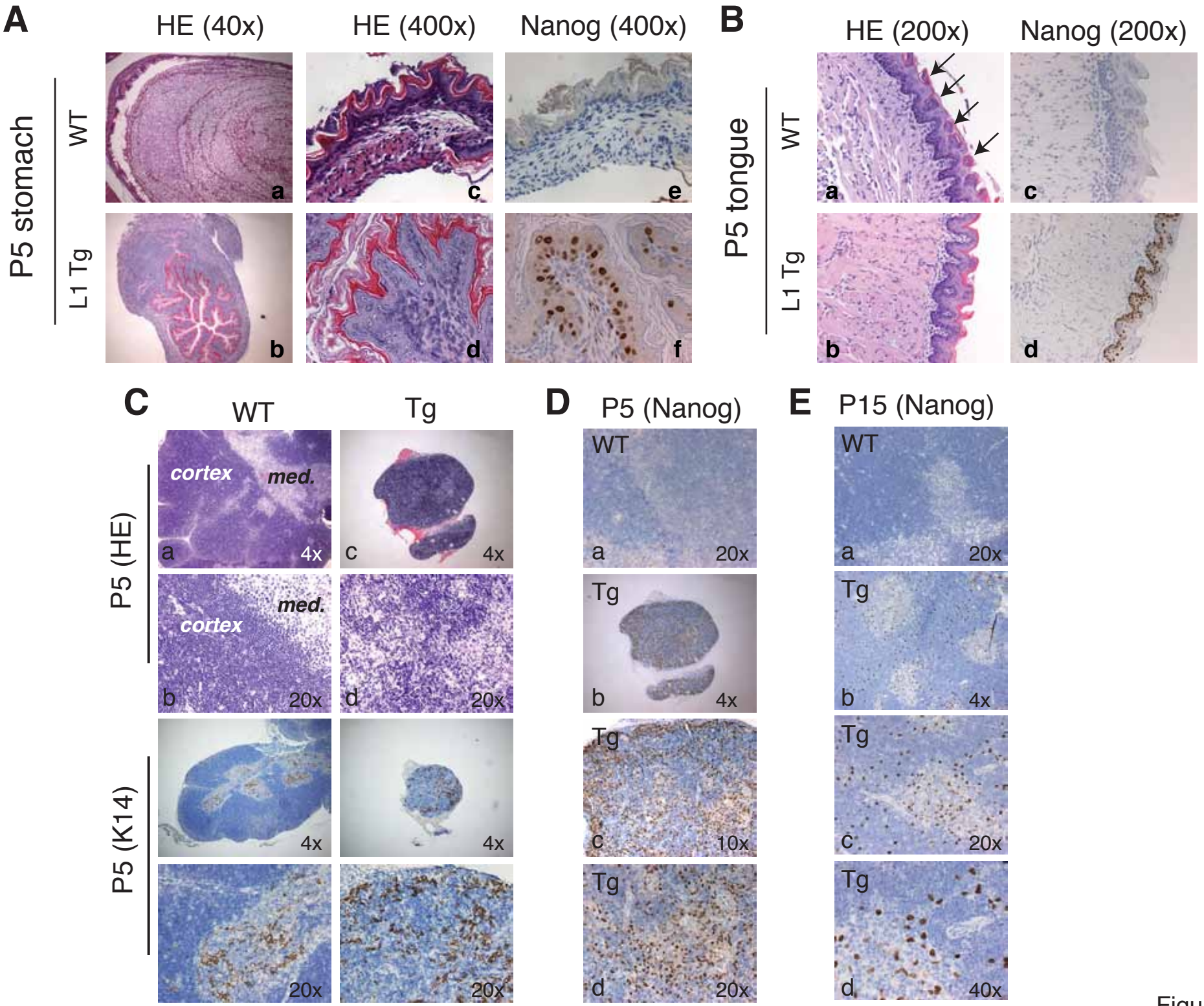
A
HE (40x)
HE (400x)
Nanog (400x)
P5 stomach
WT
L1 Tg
a
b
c
d
e
f
B
HE (200x)
Nanog (200x)
P5 tongue
WT
L1 Tg
a
b
c
d
C
WT
Tg
P5 (HE)
P5 (K14)
cortex
med.
4x
20x
D
P5 (Nanog)
WT
Tg
20x
4x
10x
E
P15 (Nanog)
WT
Tg
20x
4x
40x

Figure S3

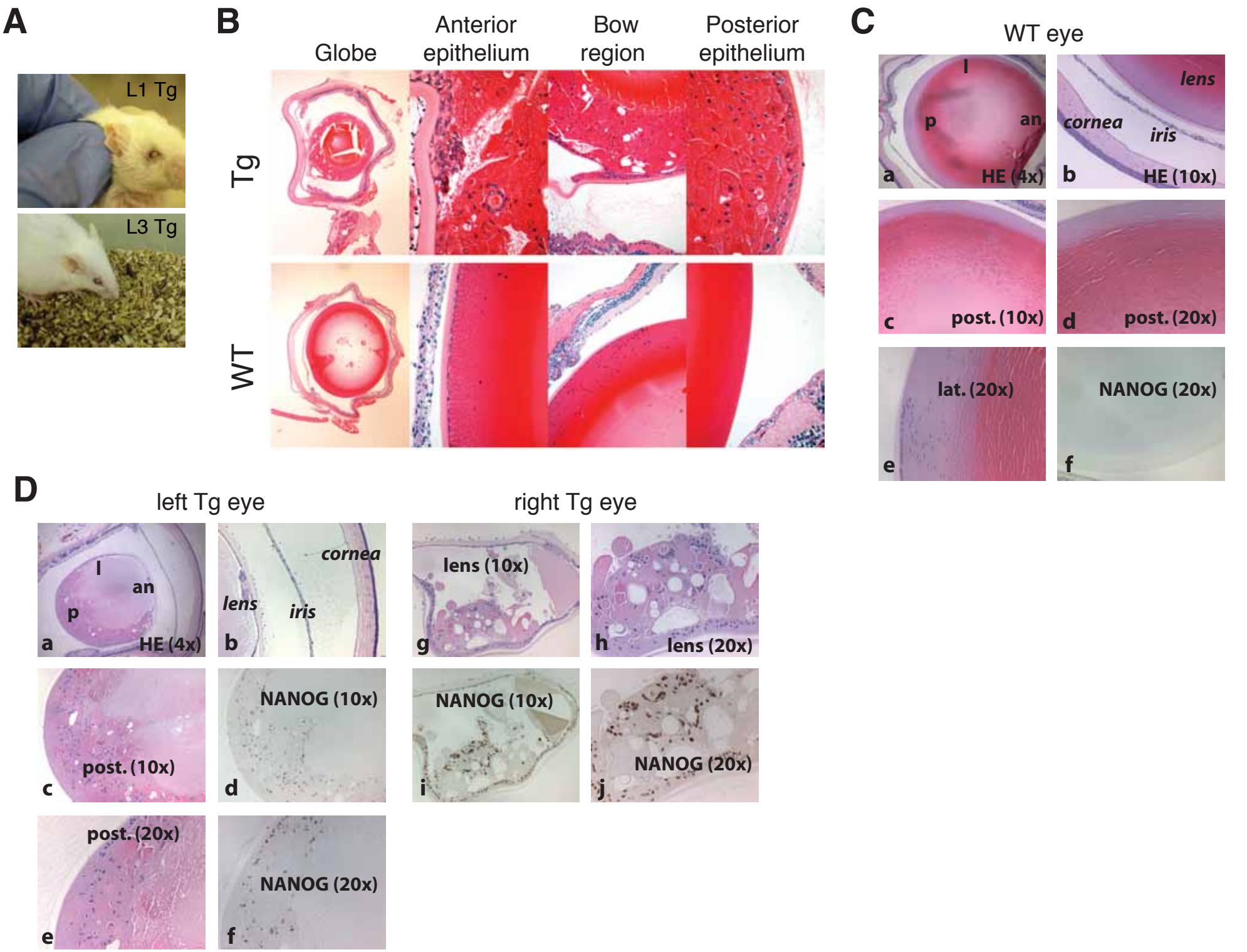
A
L1 Tg
L3 Tg
B
Globe
Anterior epithelium
Bow region
Posterior epithelium
Tg
WT
C
WT eye
l
p
an
a
HE (4x)
lens
cornea
iris
b
HE (10x)
c
post. (10x)
d
post. (20x)
lat. (20x)
e
NANOG (20x)
f
D
left Tg eye
right Tg eye
l
an
p
a
HE (4x)
cornea
lens
iris
b
lens (10x)
g
h
lens (20x)
c
post. (10x)
NANOG (10x)
d
NANOG (10x)
i
NANOG (20x)
j
post. (20x)
e
NANOG (20x)
f

Figure S4

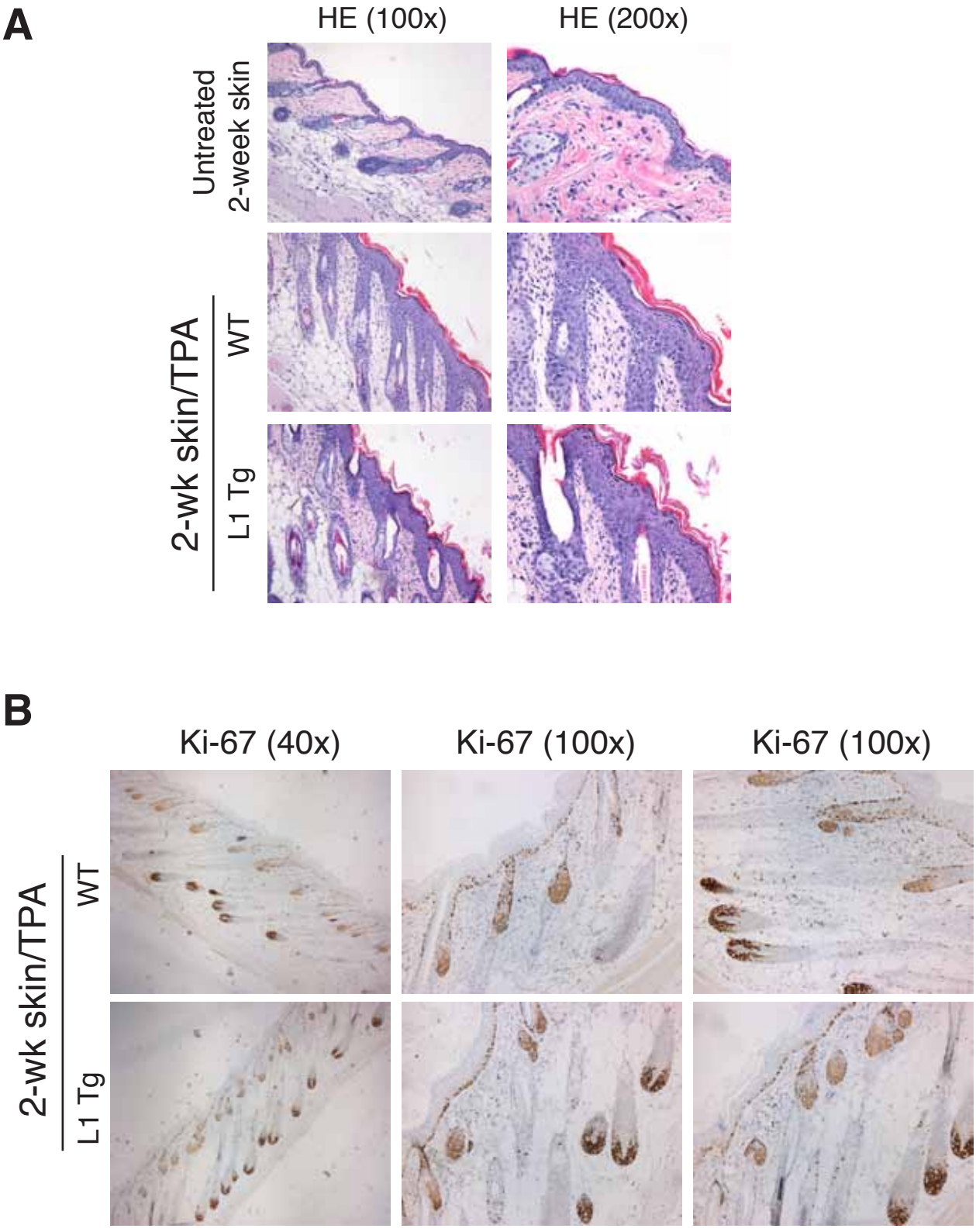
A
HE (100x)
HE (200x)
Untreated 2-week skin
2-wk skin/TPA
WT
L1 Tg
B
Ki-67 (40x)
Ki-67 (100x)
Ki-67 (100x)
2-wk skin/TPA
WT
L1 Tg

Figure S5

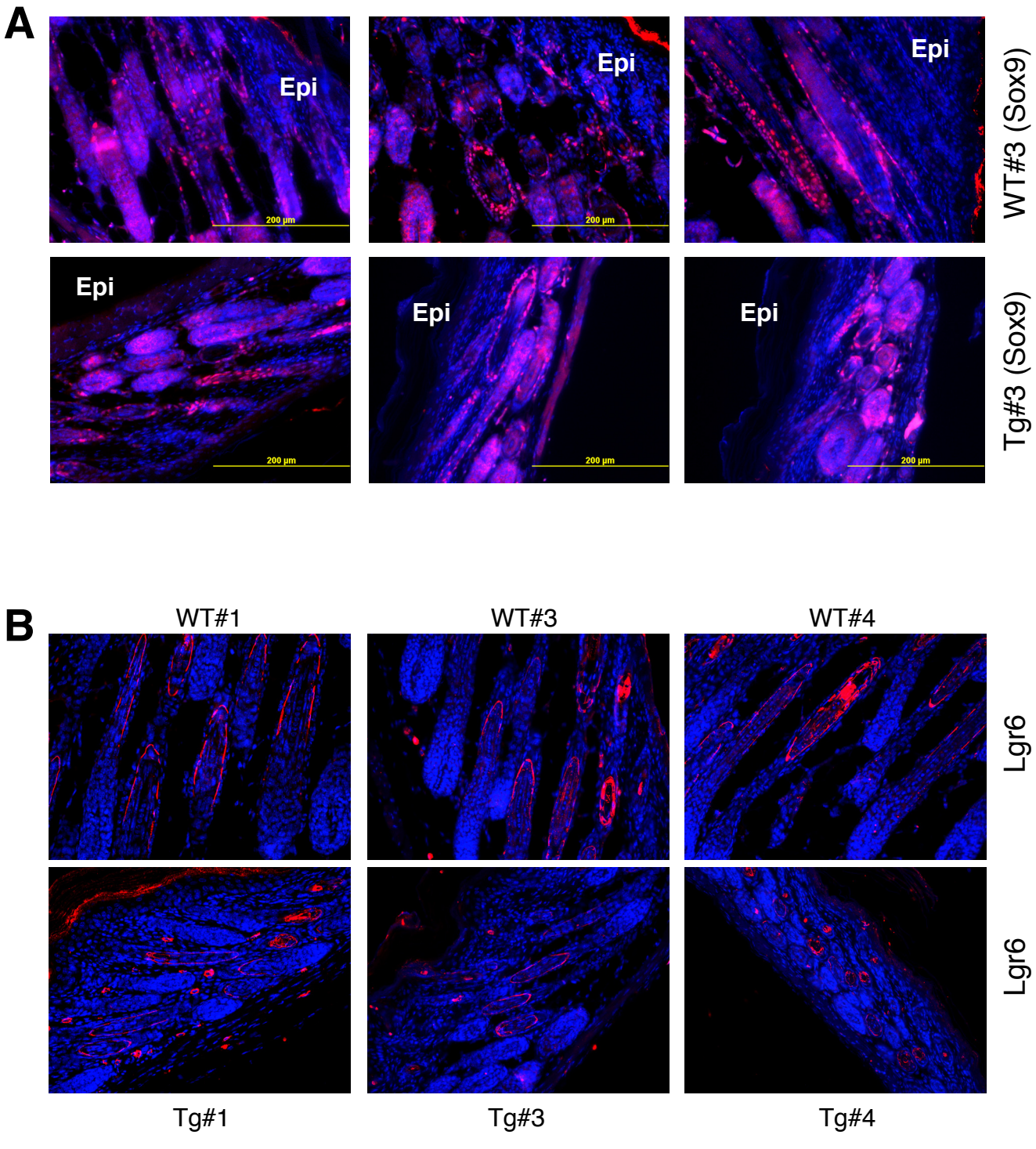
A
Epi
Epi
Epi
WT#3 (Sox9)
Epi
Epi
Epi
Tg#3 (Sox9)
200 μm
B
WT#1
WT#3
WT#4
Lgr6
Lgr6
Tg#1
Tg#3
Tg#4

Figure S6